Highlights

- Radioluminescence from α-Al_2O_3:C,Mg is reported
- The signal includes bands at 330, 410, 510, 700 and 750 nm
- The 330 nm is more prominent in annealed samples
- Both the 330 and 410 nm bands are affected by thermal quenching

F- and F^+-band radioluminescence and the influence of annealing on its emission spectra in Al_2O_3:C,Mg

M.L. Chithambo[1], J. M. Kalita[1], A.A. Finch[2]

[1]*Department of Physics and Electronics, Rhodes University, Grahamstown, South Africa*
[2]*Department of Earth & Environmental Sciences, University of St Andrews, Irvine Building, St Andrews, Fife, KY16 9AL, UK*

Abstract

Radioluminescence spectra of Al_2O_3:C,Mg monitored at temperatures up to 400°C is reported. Measurements were made on samples either *as received* or on ones annealed at 1200°C. Radioluminescence is observed at 410 nm for the unannealed sample but principally at 330 and 410 nm in the annealed sample with the emission at 330 nm dominant. Both bands are subject to thermal quenching but the change for the F^+ band is atypical. Temperature induced effects on these and other bands are discussed, as are complementary measurements of thermoluminescence spectra.

Key words radioluminescence, thermoluminescence, Al_2O_3:C,Mg, , annealing, spectra

*Corresponding author. E-mail address: m.chithambo@ru.ac.za (M.L. Chithambo).

[1] Current address: *Department of Physics, Cotton University, Guwahati -781001, India*

1. Introduction

Aluminium oxide doped with carbon and magnesium (Al_2O_3:C,Mg) is a sensitive luminescent material initially developed for optical data storage (Akselrod et al., 2003) but found suitable for neutron dosimetry (Sykora and Akselrod, 2010). The incorporation of carbon in Al_2O_3, the host, promotes within it a large concentration of electron centres notably the F-centre, an oxygen vacancy with two electrons trapped nearby, or alternatively the F^+ centre, the same point defect but with one trapped electron. These centres act as sites for thermally or optically stimulated luminescence. Although α-Al_2O_3 has emission bands near 990, 830, 410, 380 and 330 nm (Agullo-Lopez et al., 1988), the dominant ones in α-Al_2O_3:C are near 410 nm and 330 nm. Emissions near 330 and 410 nm (sometimes reported as 415 or 420 nm) are well-studied cases and are ascribed to transitions at F and F^+ point defects (McKeever et al., 1995).

When α-Al_2O_3:C is co-doped with Mg, the introduction of Mg in the matrix enhances the formation of F^+ centres, identified as F^+(Mg). A pair of adjacent F^+(Mg)-centres can form the F_2^{2+}(2 Mg) aggregate. If, during ionising irradiation, the latter traps an electron, the F_2^+(2 Mg)-centre results. Although the utility of Al_2O_3:C,Mg as a dosimeter is its main draw, the interest in this material is not restricted to this as exemplified by studies devoted to dynamics of its stimulated luminescence. For instance, Sykora and Akselrod (2010) noted emission bands at 325, 500, 510 and 750 nm using photoluminescence and attributed these to F^+(Mg), F_2, F_2^{2+}(2 Mg) and F_2^+(2 Mg) centres respectively. The thermoluminescence (TL) and phototransferred TL of Al_2O_3:C,Mg have been reported (Kalita and Chithambo, 2017a,b) as have spectral features of the TL (Kalita and Chithambo 2018a; Rodriguez et al. 2011; Trinidade and Jacobsohn, 2018). As regards radioluminescence (RL), Rodriguez et al. (2011) noted that inclusion of Mg in α-Al_2O_3:C caused new bands at 520 and 750 nm to appear in addition to pre-existing ones at 325 and 410 nm. Trinidade and Jacobsohn (2018) monitored RL at several fixed temperatures and concluded that several bands including the 410 nm (3.05 eV) one are affected by thermal quenching. Rodriguez et al. (2011) and Trinidade and Jacobsohn (2018) carried out their work on *as received* samples. In the discussion that follows, colour centres will be cited as F, F^+ etc without qualification as, say, F^+(Mg) unless otherwise stated.

We report the effect of measurement and annealing temperature on RL of principally the F and F^+ emission in unannealed and annealed Al_2O_3:C,Mg. Study of the F^+ band under stimulated emission is in some cases hampered by its transience. We thus exploit prompt emission under RL to avoid this limitation. Complementary studies by TL spectra are included. The aim of this work is to improve understanding of the dynamics of luminescence in Al_2O_3:C,Mg.

2. Experimental details

Measurements were made on Al_2O_3:C,Mg crystals of size 8 x 4 x 0.5 mm (Landauer Inc., USA). Samples were used *as received* or annealed at 1200^{o}C for 15 min owing to previous study (Kalita and Chithambo, 2018a) that showed that annealing beyond 700^{o}C causes significant change in luminescence features of Al_2O_3:C,Mg. RL and complementary TL spectra were measured in 1 mbar vacuum either at specific temperatures or during heating at 10^{o}C min^{-1} using a high sensitivity spectrometer (Luff and Townsend, 1993) now suitably upgraded (Finch et al., 2019). Samples were irradiated *in-situ* with X-rays from a Philips MCN-101 X-ray tube set at 20 kV/4 mA giving a dose rate of 1.8 Gy min^{-1}. The luminescence detection assembly consists of a combination of two spectrometers capable of recording emissions over 250-850 nm. Grating spectrometers diffract the incoming light onto position sensitive imaging detectors. The gratings disperse the signal across the relevant range i.e. 250-550 nm and 380-850 nm. All spectral data are corrected for the wavelength response of the system. A 400 nm cut-off filter is inserted in the light path to the 380-850 nm detector to remove the second order scattering of lower wavelengths into the first-order spectrum. Owing to the high sensitivity of Al_2O_3:C,Mg, neutral density filters of transmission 1% and 10% were placed in the light path to the blue and red detectors respectively.

3. Results and Discussion

3.1 Thermoluminescence spectra

3.1.1 Unannealed sample

Preparatory to RL studies, supplementary TL spectra were recorded. Figure 1 shows the spectrum of the unannealed sample measured from 30 to 400^{o}C immediately after X-ray irradiation to 3.6 Gy. The spectrum shows emission bands at 330 and 410 nm. The intense emission near room temperature is phosphorescence. This is confirmed in the inset showing a similar measurement but with a delay of 600 s between irradiation and measurement during which the phosphorescence fades.

Since the intense emission at 150^{o}C in Fig. 1 is likely to obscure the appearance of other weaker luminescence bands, a measurement tailored to better reveal the latter was made. Two spectra were obtained in succession one from 30 to 100^{o}C and the other from 100 to 180^{o}C. The sample was irradiated only once to 3.6 Gy before heating to 100^{o}C. Figure 2 (main graph) shows the spectrum for the initial measurement and for the subsequent one (inset). A glow peak at 60^{o}C (corresponding to 410 nm) now appears in addition to the previously observed prominent peak at 150^{o}C. The TL spectra of Al_2O_3:C,Mg resembles that of Al_2O_3:C reported previously (Chithambo et al., 2015). Thus the inclusion of Mg within Al_2O_3:C does not significantly alter the TL features of the unannealed host.

3.1.2 Al_2O_3:C,Mg annealed at 1200°C

In order to properly observe the TL features of the annealed sample, the corresponding spectra were measured twice consecutively. Immediately after irradiation to 0.6 Gy, the sample was heated from 30 to 200°C and, after cooling, reheated from 30 to 400°C without further irradiation. This sample was irradiated to only 0.6 Gy to avoid swamping the light detectors since it is much more sensitive than the unannealed one (Kalita and Chithambo, 2018b).

Figure 3 shows the spectrum of the annealed sample measured from 30 to 200°C and, from 30 to 400°C (inset). The emission is dominated by a band at 330 nm with the one at 415 nm just discernible. As earlier, phosphorescence is prevalent immediately after irradiation. There are glow peaks at 60 and 155°C corresponding to 330 and 410 nm emissions. There are further weaker peaks near 90°C (main plot) and 210°C (inset) both corresponding to the 330 nm band. By comparing Figs. 2 and 3, we note that the prominent emission band changes from 410 to 330 nm when the annealing temperature is increased from 20°C (denoting an unannealed sample) to 1200°C. This implies that the combination of annealing and irradiation causes an increase in the concentration of F^+ centres in a process likely to involve endothermic dissociation of F_2^{2+} aggregates to F^+ centres (Kalita and Chithambo, 2018a). F_2^{2+} centres are linked to emission at 520 nm (Rodriguez et al., 2011) which is absent or indistinct in Fig. 3.

3.2 Radioluminescence spectra

3.2.1 Spectral features of an unannealed sample

Figure 4 shows radioluminescence spectra of unannealed Al_2O_3:C,Mg measured at 30°C and 200°C (inset). The main plot shows a prominent band near 420 nm and weaker intensity one at about 510 nm. The measurement at 200°C, where the 420 nm has decreased, enables weaker emissions near 330, 510 and about 700 nm to appear. This result is consistent with that from Fig. 2 showing that under both TL and X-ray excited RL the main emission can be attributed to F-centres.

The temperature-resolved measurement of the RL is shown in Fig. 5. Such a plot is also a combination of RL and TL for deeper lying electron traps filled during X-ray irradiation as RL is measured but only emptied when the sample is heated to the activation temperature of these electron traps. Figure 5 shows intense emission at ~410 nm between 30 and 120°C. The emission goes through a peak at 155°C reflecting the existence of a glow peak here as noted earlier for Fig. 2. The measurement from 200 to 400°C (inset) shows other bands with the one at 700 nm clearer.

The luminescence emitted at 695 nm (noted at 700 nm in Fig. 5) has previously been reported in Cr-doped Al_2O_3 e.g. (Chandler and Townsend, 1979) as well as in Cr-doped beryl (Chithambo et al., 1995). The emission is associated with Cr^{3+} which substitutes for Al^{3+}. The emission comprises a sharp R_1 and R_2 doublet which is better apparent at low temperature

(Chithambo et al., 1995). The emission appears broad since it is a composite of the $^2E \rightarrow {}^4A_2$ and $^4T_2 \rightarrow {}^4A_2$ transitions. Our previous study on the composition heterogeneity of Al_2O_3:C, the host, identified Cr to be present as a trace impurity or in Cr-bearing phases such as Cr-bearing magnetite or Cr-bearing hercynite (Chithambo and Costin, 2017).

3.2.2 Spectral features of an Al_2O_3:C,Mg annealed at 1200°C

Figure 6 shows the temperature dependence of RL for the annealed sample. Bands near 330 and 410 nm are apparent with the one at 330 nm prominent. Figure 6(inset i) compares RL obtained at 30°C (yellow circles) and at 200°C. Both bands decrease in intensity with measurement temperature but more so at 410 nm. The well-known decrease for the latter reflects thermal quenching at the F centre (McKeever et al., 1995). The change for the F^+ band suggests that it may involve other processes other than thermal quenching alone as the decline in intensity with temperature would otherwise be greater. Inset (ii) is included to show other bands that are otherwise obscured by the more intense 330 and 410 nm emissions. Of particular interest is the emission at 750 nm which appears in both the annealed and unannealed sample (at 750 nm). The latter is ascribed to the F_2^+ centre and is also known to be transient. We surmise that under RL, the 750 nm band increases in importance at the expense of the 510 nm one owing to radiolytic transformation of F_2^{2+} to F_2^+ centres.

3.3 The influence of measurement temperature on RL spectra

The RL intensity monitored from an unannealed sample at 410 nm at specific temperatures from 40 to 260°C and from 260 to 40°C (solid circles) immediately thereafter is shown in Fig. 7. In both cases, the RL intensity is comparable within statistical scatter below 150°C but decreases consistently from 150 to 260°C. The intensity of RL measured with the temperature decreasing exceeds that in the initial run likely because there is no competitive retrapping into lower-temperature-lying electron traps. For the latter, the dependence of intensity $I(T)$ on temperature better follows the typical behaviour of $I(T) = I_{rad}/(1 + Cexp(-\Delta E/kT))$ where T is the absolute temperature, I_{rad} is the intensity at 0 K, ΔE is the activation energy for thermal quenching, k is Boltzmann's constant and the constant C is equal to $\nu\tau_{rad}$ where ν is the frequency factor for the non-radiative process e.g. (Chithambo et al., 2015). The solid line through data is the best fit of $I(T)$ giving $\Delta E = 0.90 \pm 0.02$ eV. This value is consistent with the one reported by Kalita and Chithambo (2017a).

Figure 7 (inset) shows results for the annealed sample. Although for this sample, the emission at 330 nm is more prominent than that at 410 nm, both were studied. The intensity of the 330 nm emission (solid inverted triangles) decreases monotonically. While the change at 410 nm (open inverted triangles) is archetypal, that at 330 nm is not. One can forward several reasons for this. If the number of F^+ centres responsible for the 330 nm emission increases by radiolytic transformation of F_2^{2+} centres, it would ameliorate against the decrease in intensity due to thermal quenching and cause the observed change to be spuriously slow. The typical account for thermal quenching is based on transition of an electron from an excited

state to another (that is degenerate to both the ground and the excited states) from which a radiationless transition to the ground state occurs (Chithambo et al., 2015). The F^+ has a 3-fold degenerate excited state with three absorption bands at 6.3, 5.41 and 4.84 eV (Agullo-Lopez et al., 1988) although the emission at 330 nm (3.76 eV) is attributed to a transition from its 1B excited state to the 1A ground state (Agullo-Lopez et al., 1988). The specifics of thermal quenching in such a system are yet to be worked out but this exercise is beyond the scope of this report.

4. Conclusion

The radioluminescence of α-Al_2O_3:C,Mg either annealed at 1200^{o}C or used *as received* is reported. RL is prominent at 410 nm for the unannealed sample but principally at 330 and 410 nm when the sample is annealed at 1200^{o}C with the emission at 330 nm dominant. Both bands are subject to thermal quenching but the change for the F^+ band is atypical.

Acknowledgements

We are grateful to Rhodes University and the National Research Foundation of South Africa for financial support.

References

Agullo-Lopez, F., Catlow, C.R.A., Townsend, P.D., 1988. Point defects in materials, Academic Press, London.

Akselrod, M.S., Akselrod, A.E., Orlov, S.S., Sanyal, S., Underwood, T.H., 2003. Fluorescent aluminum oxide crystals for volumetric optical data storage and imaging applications. J. Fluores. 13, 503-511.

Akselrod, M.S, Yoder, R.C., Akselrod, G.M., 2006 Confocal fluorescent imaging of tracks from heavy charged particles utilising new Al_2O_3:C,Mg crystals, Radiat. Prot. Dosim, 119, 357–362.

Chandler, P.J., Townsend, P.D., 1979. Implantation temperature measurement using impurity luminescence, Radiat. Eff. Defect. Solid. 43, 61-64.

Chithambo, M.L., Costin, G., 2017. Temperature-dependence of time-resolved optically stimulated luminescence and composition heterogeneity of synthetic a-Al_2O_3:C. J. Lumin. 182, 252-262.

Chithambo, M.L., Nyirenda, A.N., Finch, A.A., Rawat, N.S., 2015. Time-resolved optically stimulated luminescence and spectral emission features of α-Al_2O_3:C, Physica B, 473, 62–71.

Chithambo, M.L., Raymond, S.G., Calderon, T., Townsend, P.D., 1995. Low temperature luminescence of transition metal-doped beryls, J. African Earth Sci. 20, 53-60.

Finch, A.A., Wang, Y., Townsend, P.D., Ingle, M., 2019. A high sensitivity system for luminescence measurement of materials Luminescence. J. Bio. Chem. Lumin. 34, 280-289.

Kalita, J.M., Chithambo, M.L., 2017a. Comprehensive kinetic analysis of thermoluminescence peaks of α-Al_2O_3:C,Mg. J. Lumin 185, 72-82.

Kalita, J.M., Chithambo, M.L., 2017b. Phototransferred thermoluminescence in α-Al_2O_3:C,Mg under 470 nm blue light stimulation. J. Lumin. 188, 371-377.

Kalita, J.M., Chithambo, M.L., 2018a. The effect of annealing and beta irradiation on thermoluminescence spectra of α-Al_2O_3:C,Mg, J. Lumin. 196, 195–200.

Kalita, J.M., Chithambo, M.L., 2018b. Thermoluminescence of α-Al_2O_3:C,Mg annealed at 1200 °C, Nucl. Inst. Method. Phys. Res. B, 422, 78–84.

Luff, B.J., Townsend, P.D., 1993. High sensitivity thermoluminescence spectrometer, Meas. Sci. Technol. 4, 65-71.

McKeever, S.W.S., Moscovitch, M., Townsend, P.D., 1995. Nuclear Technology Publishing, Kent, UK.

Rodriguez, M.G., Denis, G., Akselrod, M.S., Underwood, T.H., Yukihara, E.G., 2011. Thermoluminescence, optically stimulated luminescence and radioluminescence properties of Al_2O_3:C,Mg, Radiat. Meas. 46, 1469-1473.

Sykora, G.J., Akselrod, M.S., 2010. Photoluminescence study of photochromically and

radiochromically transformed Al_2O_3:C,Mg crystals used for fluorescent nuclear track detectors, Radiat. Meas. 45, 631–634.

Trindade, N.M., Jacobsohn, L.G., 2018. Thermoluminescence and radioluminescence of α-Al_2O_3:C,Mg at high temperatures, J. Lumin. 204, 598–602.

Figure captions

Figure 1. Thermoluminescence spectra of unannealed Al_2O_3:C,Mg measured immediately after irradiation (main graph) and after 600 s delay between irradiation and measurement (inset).

Figure 2 Thermoluminescence spectra of unannealed Al_2O_3:C,Mg between 30-100^oC (main graph) and 100-180^oC (inset).

Figure 3 Thermoluminescence spectra of the annealed sample measured from 30 to 200^oC and, from 30 to 400^oC (inset).

Figure 4 Radioluminescence spectra of unannealed Al_2O_3:C,Mg measured at 30^oC and, 200^oC (inset).

Figure 5 Radioluminescence spectra measured between 30 and 400^oC as shown.

Figure 6 Temperature dependence of RL for the annealed sample. Inset (i) shows RL obtained at 30^oC (yellow symbols) and at 200^oC. Inset (ii) highlights weaker bands.

Figure 7 Radioluminescence monitored at 410 nm against temperature in an unannealed sample. The inset are results for the annealed sample. The dotted lines are visual guides.

Figure 1

Click here to access/download;Figure;Figure 1.jpg

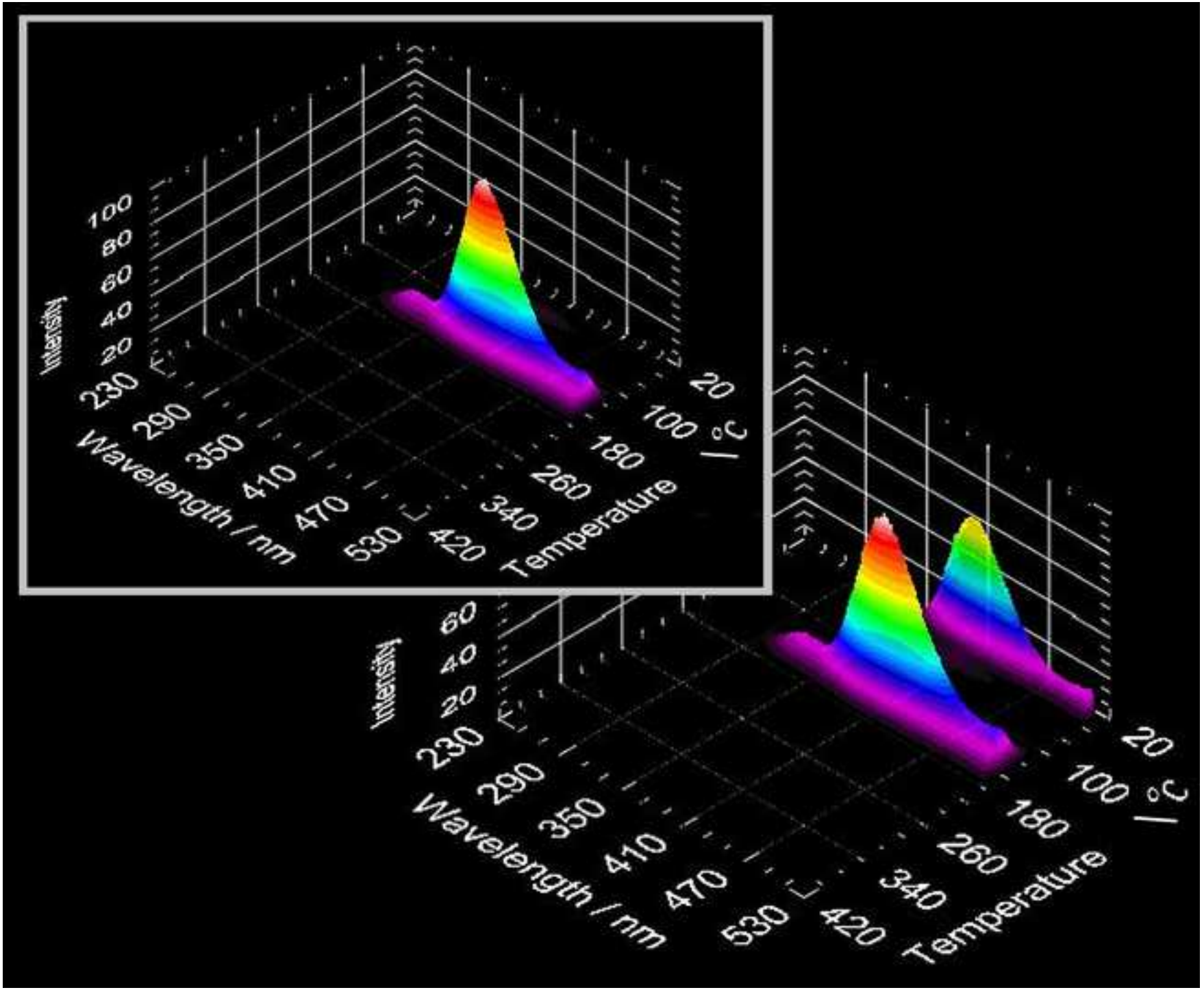

Figure 2

Click here to access/download;Figure;Figure 2.jpg

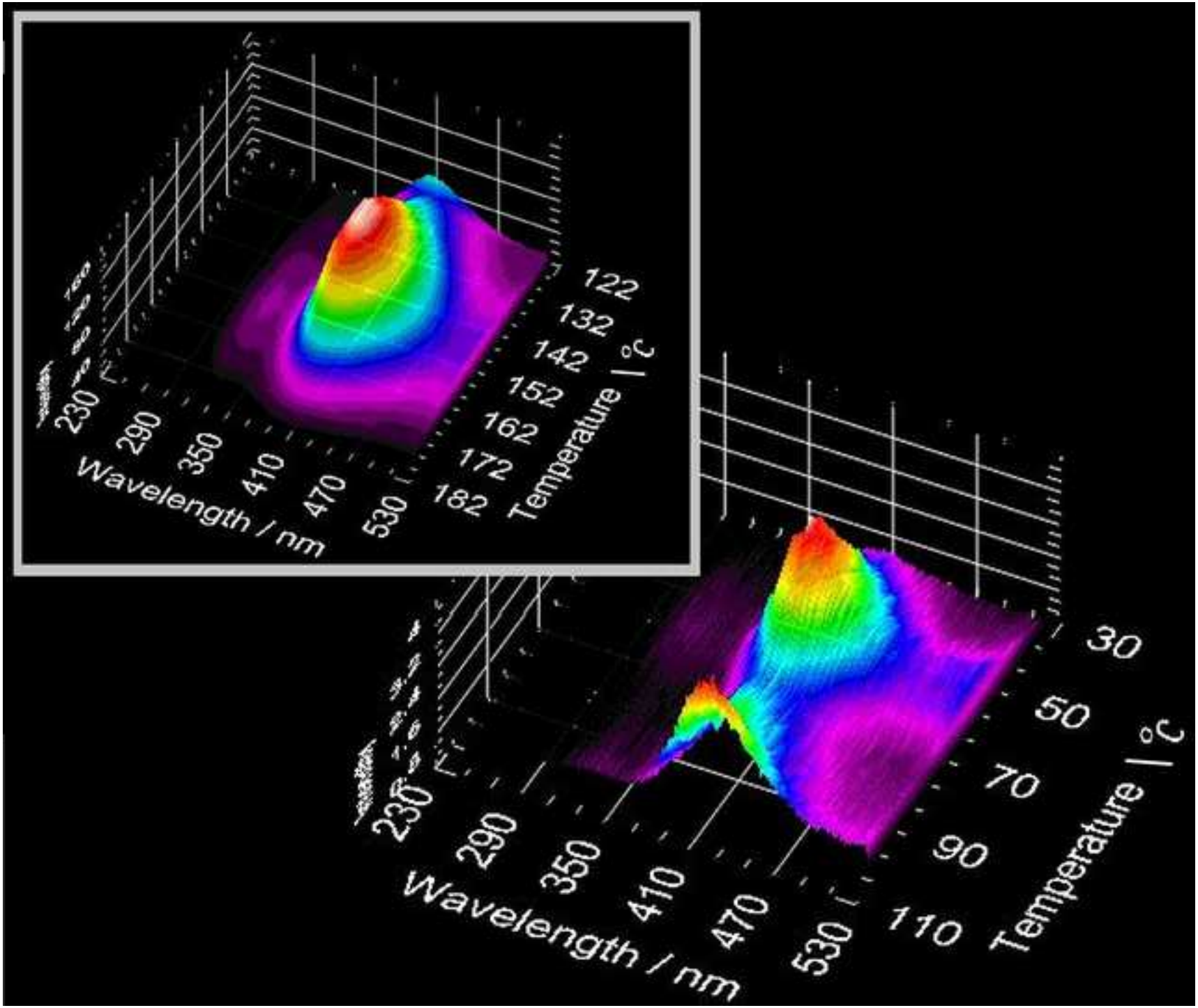

Figure 3

Click here to access/download;Figure;Figure 3.jpg

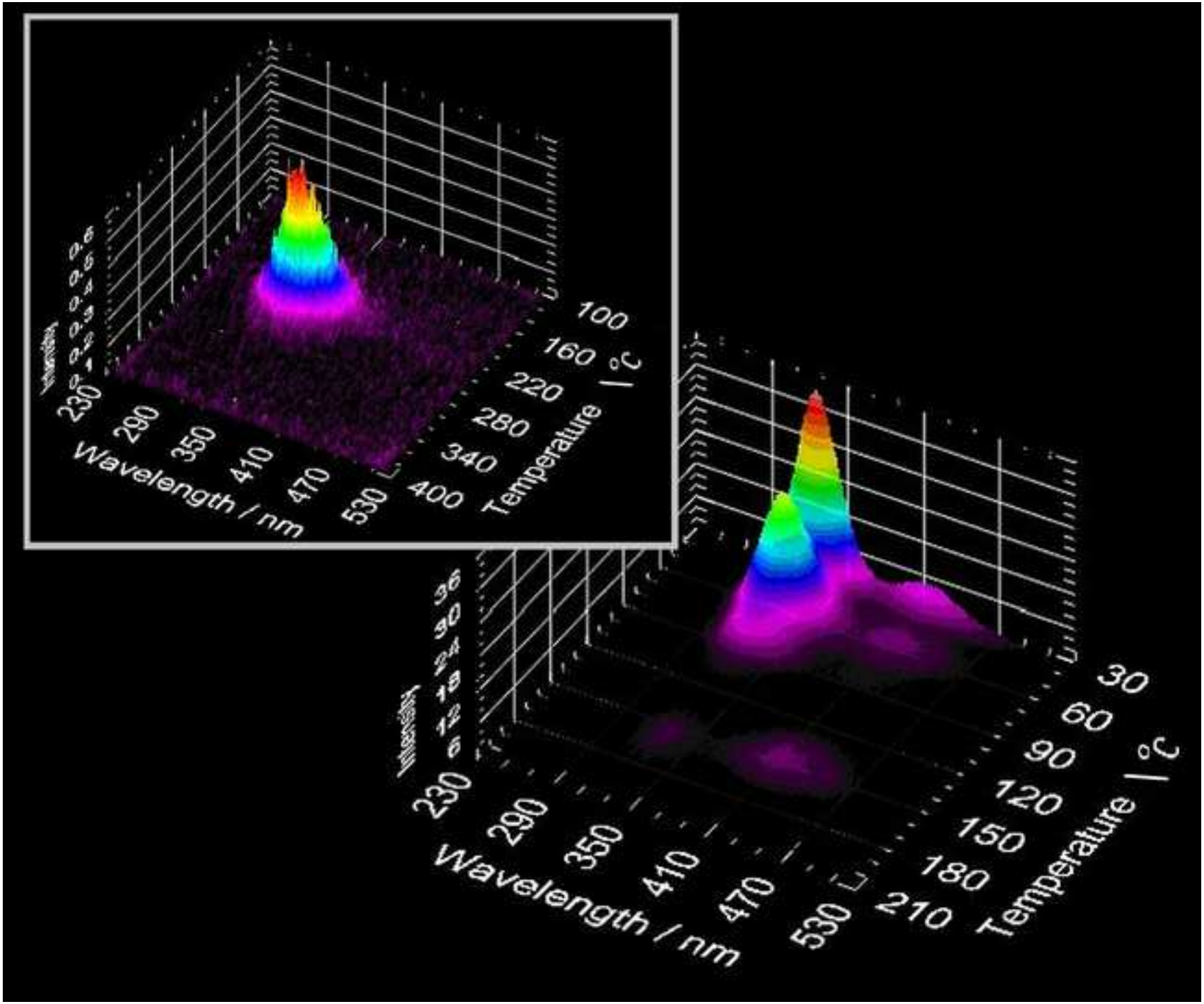

Figure 4

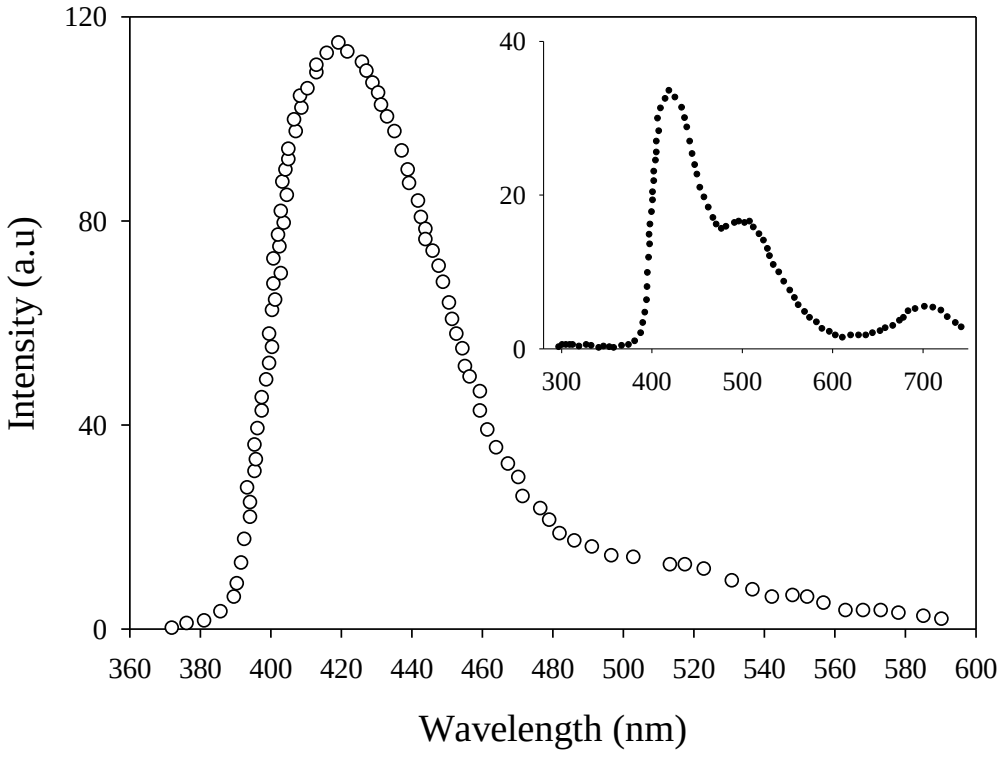
120
80
40
0
Intensity (a.u)
360
380
400
420
440
460
480
500
520
540
560
580
600
Wavelength (nm)
40
20
0
300
400
500
600
700

Figure 5

Click here to access/download;Figure;Figure 5.jpg

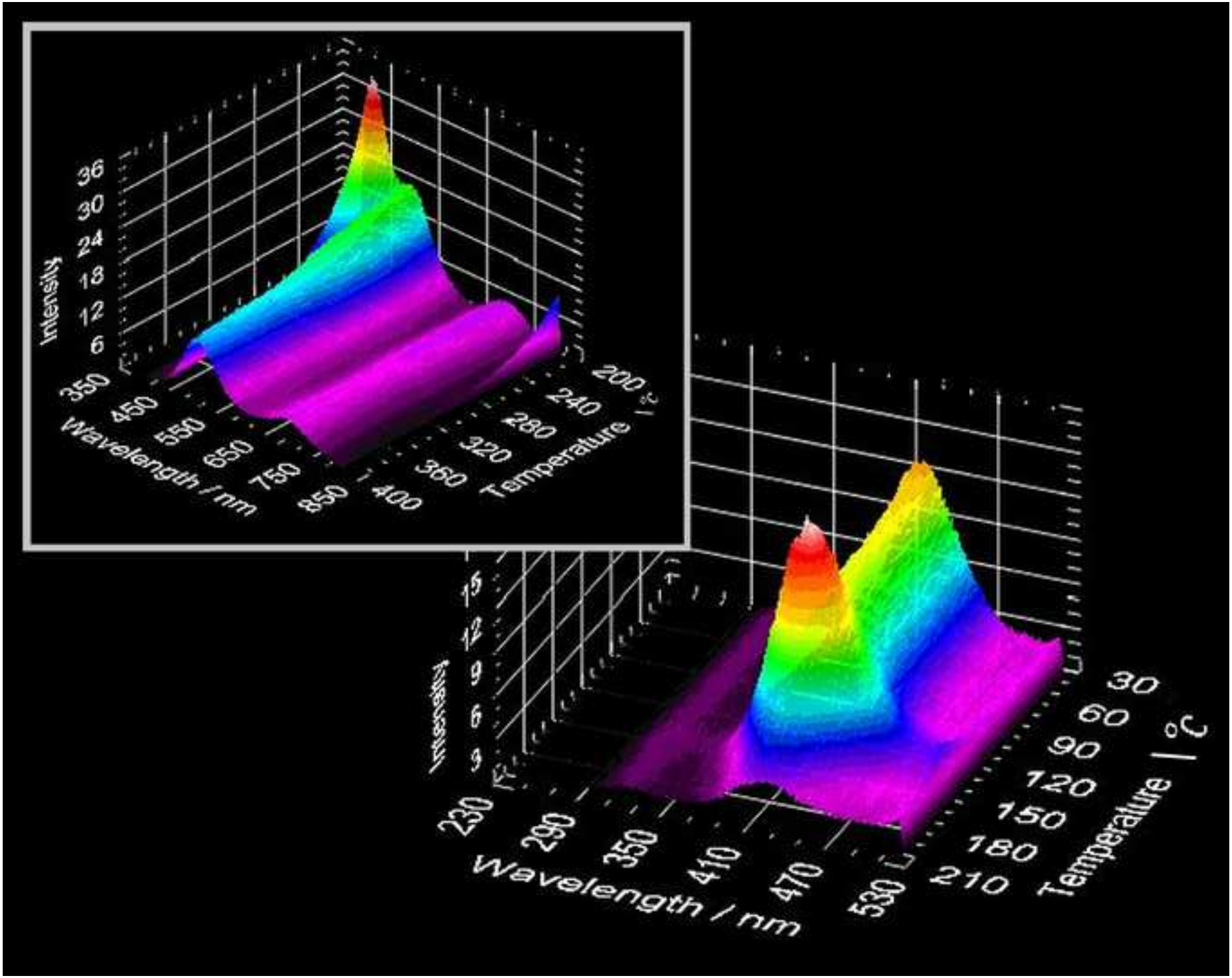

Figure 6

Click here to access/download;Figure;Figure 6.jpg

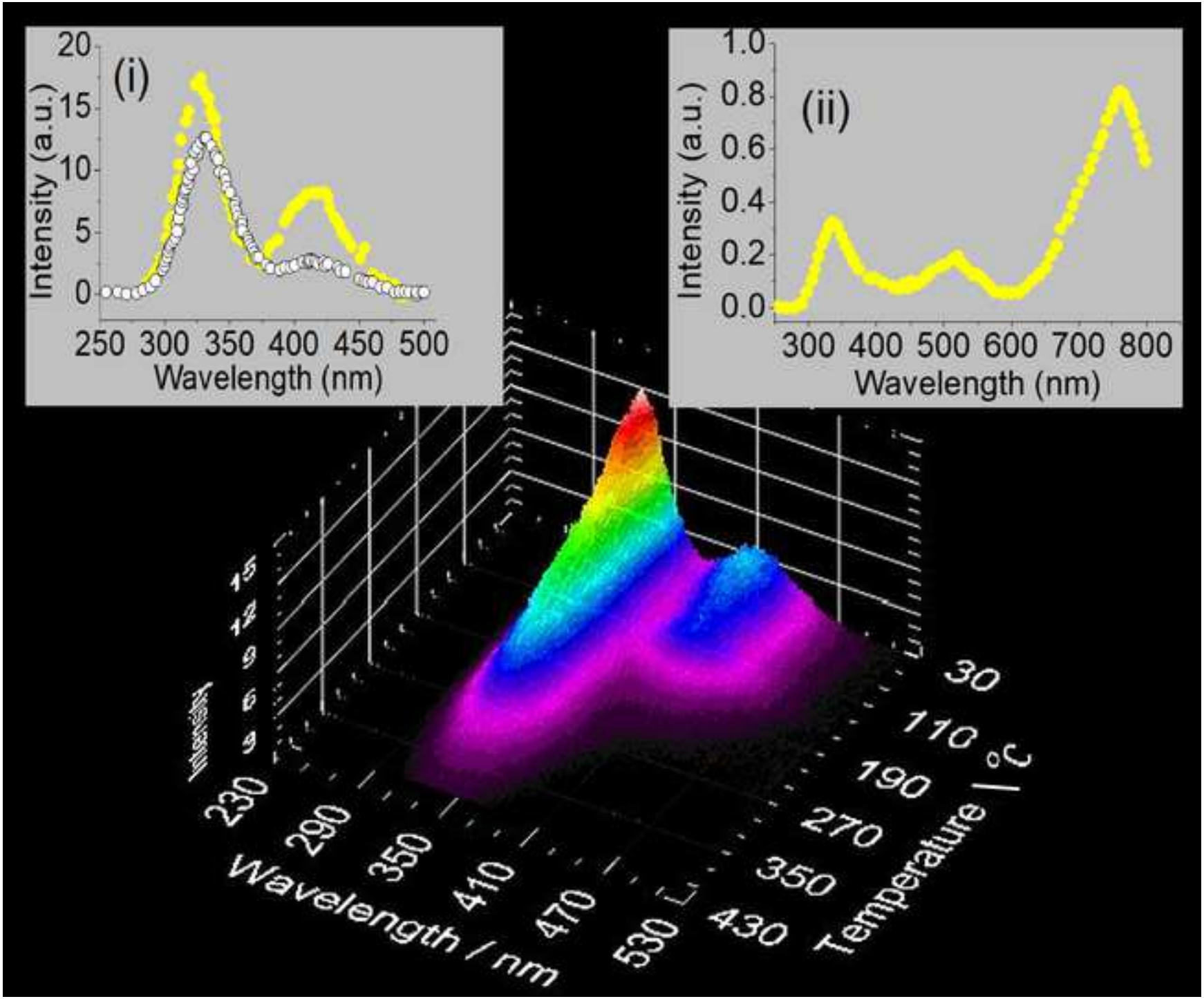

Figure 7

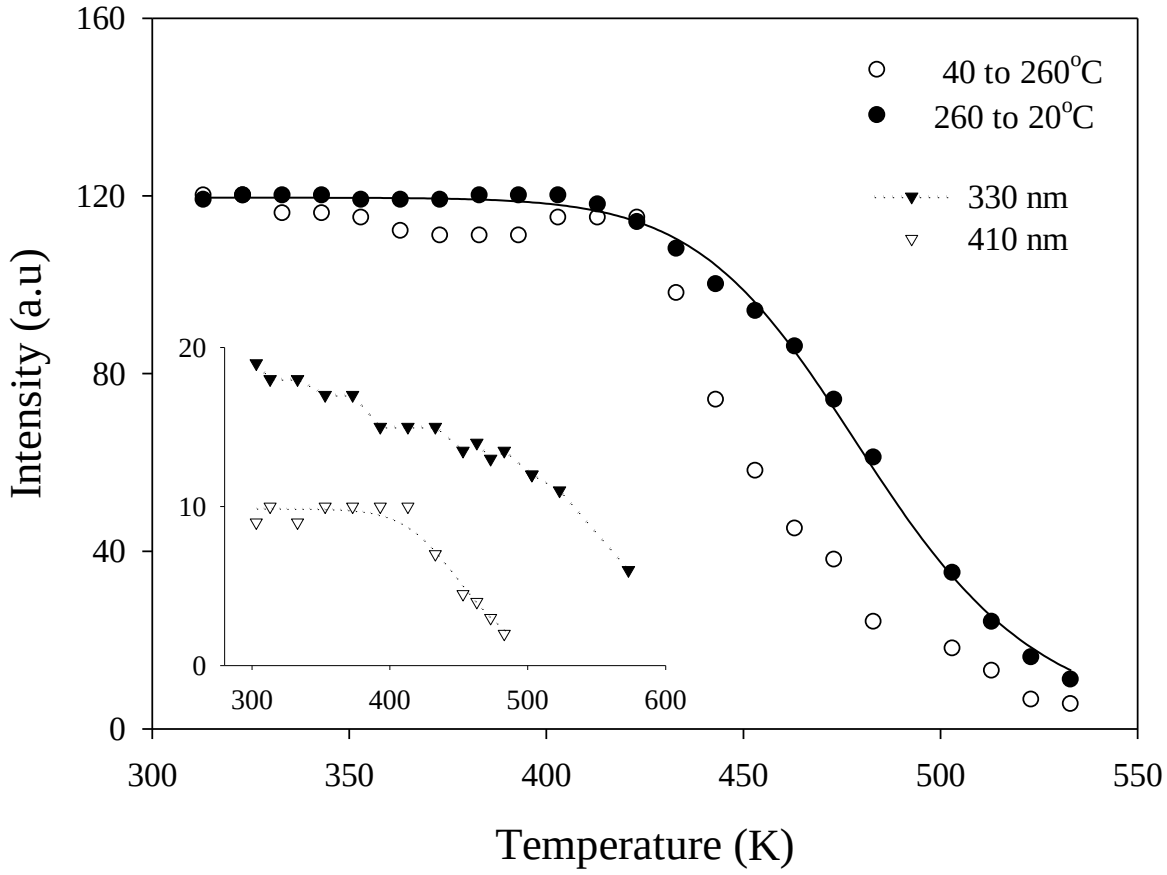
160
120
80
40
0
Intensity (a.u)
300
350
400
450
500
550
Temperature (K)
40 to 260°C
260 to 20°C
330 nm
410 nm
20
10
0
300
400
500
600